Supporting Information

Reduced methylammonium, triple-cation $Rb_{0.05}(FAPbI_3)_{0.95}(MAPbBr_3)_{0.05}$ perovskite solar cells based on TiO_2/SnO_2 bilayered electron transporting layer approaching 21% efficiency: Role of TFT antisolvent

Sawanta S. Mali,[a] Jyoti V. Patil,[a] Hamidreza Arandiyan,[b] Chang Kook Hong*[a]

Materials and Methods

Materials

All of the chemicals and materials were purchased and used without further purification. Materials including solvents (N, N-Dimethylformamide (DMF), Dimethyl sulfoxide (DMSO), diethyl sulfide (98%), PbI_2 (99%), RbI (99.9% Sigma-Aldrich) and tin(II) chloride hydrate ($SnCl_2 \cdot 2H_2O$, >98 %, Sigma-Aldrich) were purchased from Sigma-Aldrich and used as received. Hydroiodic acid (aqueous, 57 wt %, Sigma-Aldrich) to a solution of methylamine (aqueous, 40 wt %, TCI Chemicals), formamidine acetate (Sigma-Aldrich) was used for preparation of MAI, FAI. For HTM preparation toluene (99%, Sigma Aldrich), acetonitrile (99.8% Sigma-Aldich) and 4-tert-butylpyridine (TBP, 96%, Aldrich) solvents were used. Antisolvents such as chlorobenzene (CB, >99 % Sigma Aldrich), diethyl-ether (>99 % Sigma Aldrich) and α,α,α-Trifluorotoluene (TFT, >99% Sigma-Aldrich) have been used as received.

Methods

Preparation of c-TiO_2 and TiO_2/SnO_2 bilayer Electron transport layer (ETL)

Laser-patterned FTO-coated glass substrates (TEC-8, Philkington) were ultrasonically cleaned in an alkaline aqueous solution, rinsed with deionized water, acetone, ethanol and then treated with UV-ozone for 15 min. Nearly 60-80 nm thin compact blocking TiO_2 (Bl-TiO_2) layer was deposited on the substrates by spin coating the TiO_2 precursor and then annealing the spin-coated precursor in air at 450 °C for 30 min. The precursor composition was as follows: 1 ml commercial titanium isopropoxide solution (Sigma-Aldrich) that was diluted in ethanol containing 12M HCl. The SnO_2 bilayer on TiO_2 ETL was achieved by using 0.05 M tin (II) chloride hydrate [$SnCl_2.2H_2O$] in ethanol was spin coated at 3000 rpm for 20 sec followed by 45 min annealing at 180 °C.

Synthesis of the perovskite precursors and their solution

The FAI, MABr were synthesized as per our reports.[S1, S2] Briefly, methylamine solution, formamidine acetate powder were separately reacted with hydroiodic acid (57%in water, Aldrich) and hydrobromic acid (HBr) for the preparation of MABr and FAI. The reactions were carried out in a 250 ml round-bottomed flask at 0°C for 2 h with stirring. The precipitates were recovered by evaporating the solutions at 60°C for 2 h. The products were dissolved in ethanol or methanol, recrystallized using diethyl ether, and finally dried at 60 °C in a vacuum oven for 24 h. For FAPbX/MAPbX precursors was synthesized by reacting FAI, MABr, PbI_2, and $PbBr_2$ powder with desired amount in DMF/DMSO (4:1 v/v%) solution. Desired volume (5%) of RbI in DMF:DMSO (4:1) was added in above solution to make $Rb_{0.05}[(FAPbI_3)_{0.95}(MAPbBr_3)_{0.05}]_{0.95}$. The clear filtered yellow solution was spin coated on the top of the FTO/TiO_2 as well as FTO/TiO_2/SnO_2 ETLs by a consecutive two-step spin coating process at 1,000 and 6,000 rpm for 10 and 30 s, respectively. 100 μl of CB, 1 ml diethyl-ether or 200 μl of TFT was drop-cast during the second spin-coating step followed by a heat treatment (130°C) on a hot plate for 10 min to form dark-black colored crystalline $Rb_{0.05}(FAPbI_3)_{0.95}(MAPbBr_3)_{0.05}$ thin film.

Preparation of PTAA based HTM

The hole transport material (HTM) was prepared by as per our previous report [S3]. The 15 mg of a poly[bis(4-phenyl)(2,4,6-trimethylphenyl)amine] (PTAA, sigma Aldrich) dissolved in 1.5 mL toluene (99.8%, Aldrich) with addition of 15 μL bis(trifiuoromethane) sulfonimide lithium salt (LiTFSI, 99.95%, Aldrich) (170mgml^{-1}) in acetonitrile and 7.5 μL 4-tert-butylpyridine (TBP, 96%, Aldrich). The prepared PTAA HTM solution was spin-coated on the FTO/TiO_2/SnO_2/perovskite electrode at 3,000 rpm for 30s. Then the substrates were transferred to a vacuum chamber and evacuated to a pressure of 2×10^{-6} mbar. For the counter

electrode, a 80 nm thick Au contacts were deposited on the top of the HTM over layer by a thermal evaporation (growth rate ~0.5Å/s). Precaution was taken for each step as per previous literature. The active area of this electrode was fixed at 0.09 cm^2. An active area was calculated as per gold and laser pattern cross-sectional area. The exact illumination to the active area was fixed by attaching metal shadow mask from back side during measurements.

Characterizations

The top-surface and cross-sectional images were recorded by a field emission scanning electron microscope (FESEM; S-4700, Hitachi). X-ray diffraction (XRD) measurements were carried out using a D/MAX Uitima III XRD spectrometer (Rigaku, Japan) with Cu K line of 1.5410 Å. The photoluminescence (PL) spectra were measured using photoluminescence spectrometer (f=0.5m, Acton Research Co., Spectrograph 500i, USA), and an intensified CCD(PI-MAX3) (Princeton Instrument Co., IRY1024, USA). The DPSS (Diode pumped solid state) laser (Ekspla) with a wavelength of 266 nm and a power of 310 mW was utilized as an excitation source for PL measurement.

Photovoltaic studies

The cells were illuminated using a solar simulator at AM 1.5 G for 10 s, for which the light intensity was adjusted to 1 sun intensity (100 mW cm^{-2}) through the use of an NREL-calibrated Si solar cell with a KG-5 filter. The spectral response was taken by an spectral IPCE measurement system (K3100, McScience), which was equipped with a monochromator, a K240 XE 300 lamp source connected with K401 OLS XE300W lamp Power supply and a K102 Signal amplifier. Prior to the use of the light, the spectral response and the light intensity were calibrated using a Si-photodiode (Model: S1337-1010BQ) and InGaAs photodiode (model: G12180-050A) for 300-1100 nm and 1100-1400 nm calibration respectively. Measurements were taken in EQE mode.

Time-resolved photoluminescence (PL) decay transients were measured at 800±20nm using excitation with a 470 nm light pulse at a frequency of 5MHz from the Spectrophotometer F-7000.

Device stability

The device stability was tested in air at 80 °C without any encapsulation.

Figure S1 (a,b) Cross sectional SEM micrographs of monolayer TiO_2 and TiO_2/SnO_2 bilayer ETL, (c,d) respective perovskite precursor solution contact angle

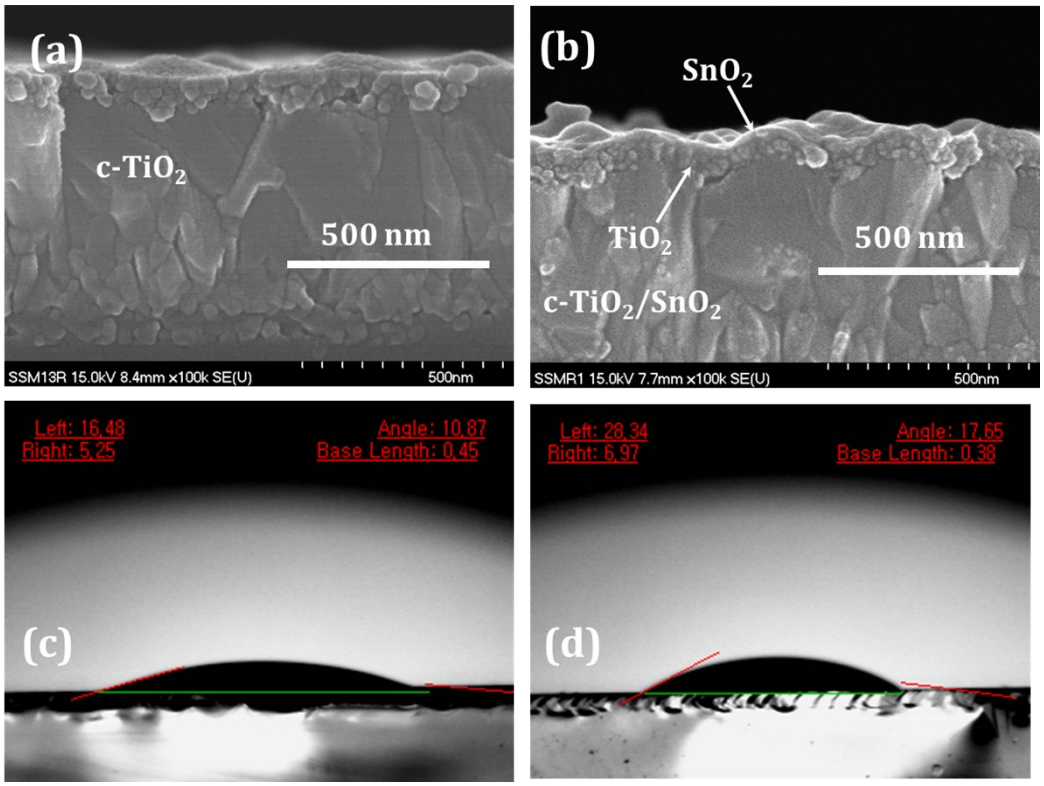

Fig. S2 Survey spectrum of c-TiO_2 and TiO_2/SnO_2 bilayer ETL thin films.

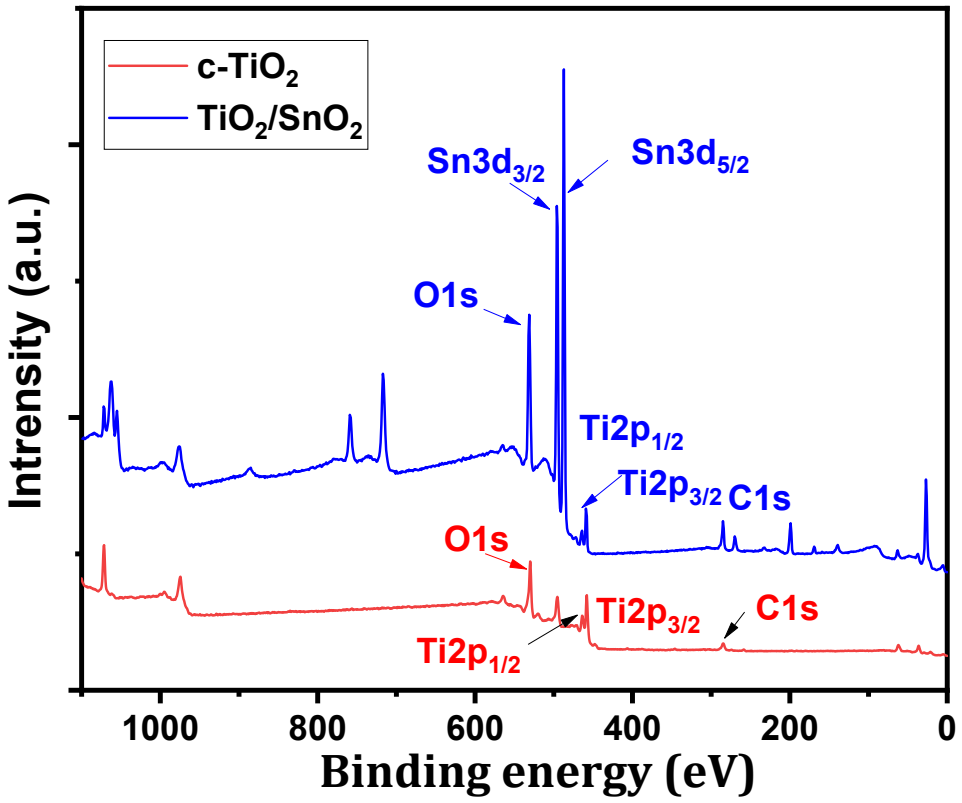

Figure S3a Top-view and cross sectional micrographs of Perovskite thin film deposited by using different antisolvent on single and bilayer ETL.

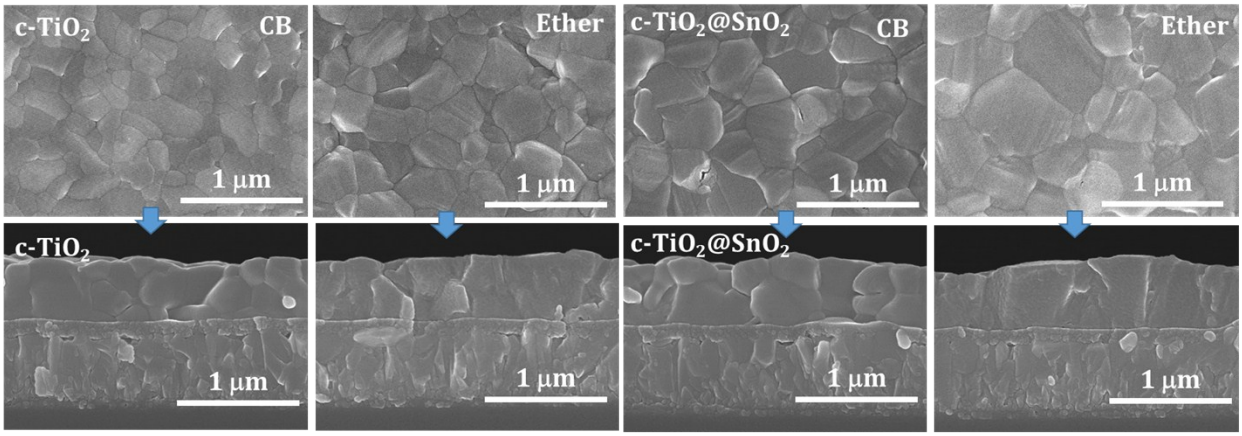

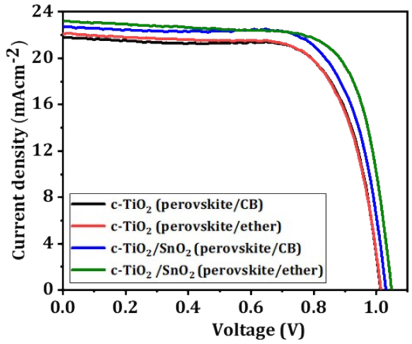

ETL	Antisolvent	V_{OC} (V)	J_{SC} ($mAcm^{-2}$)	FF (%)	PCE (%)
c-TiO_2	CB	1.009	21.77	71.05	15.60
	Diethyl ether	1.018	22.15	72.30	16.30
c-TiO_2/SnO_2	CB	1.029	22.74	71.82	16.80
	Diethyl ether	1.045	23.13	73.42	17.74

Figure S3b Low-magnification top-view micrograph of Perovskite thin film deposited on c-TiO_2/SnO_2 ETL bilayer ETL with TFT anti-solvent.

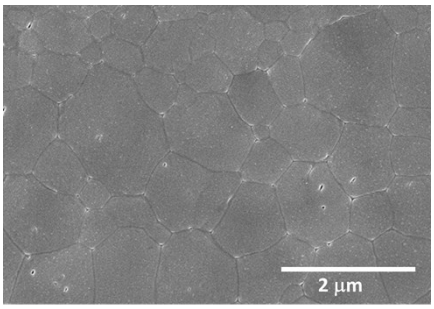

Fig. S4 XRD patterns of $FAPbI_3$ perovskite and its conventional mixed composition with ratio 0.85:15 (FA:MA) and modified 0.95:0.05 (FAMA) for fresh and annealing at 130 °C for 3 hours.

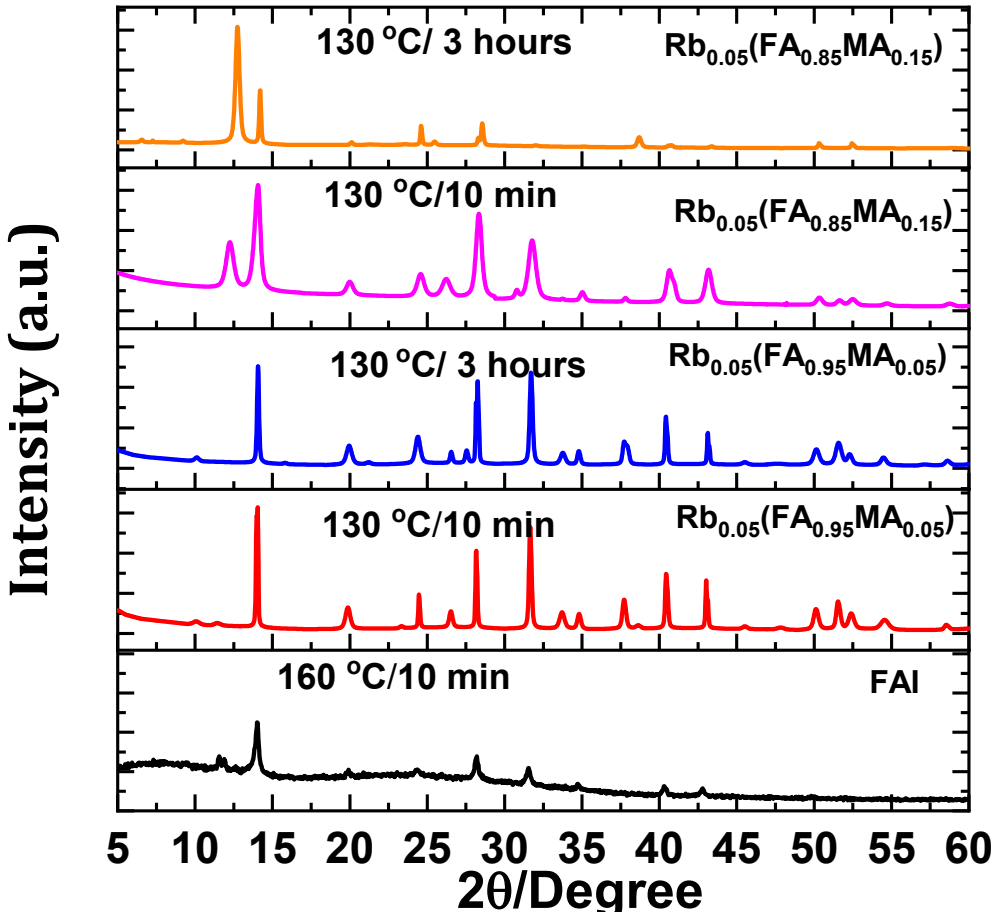

Fig. S9 Thermal-stability at 80 °C at 35 % RH of $(FAPbI_3)_{0.85}(MAPbI_3)_{0.15}$ and $Rb_{0.05}(FAPbI_3)_{0.85}(MAPbI_3)_{0.15}$ composition for bilayered ETL based perovskite solar cells

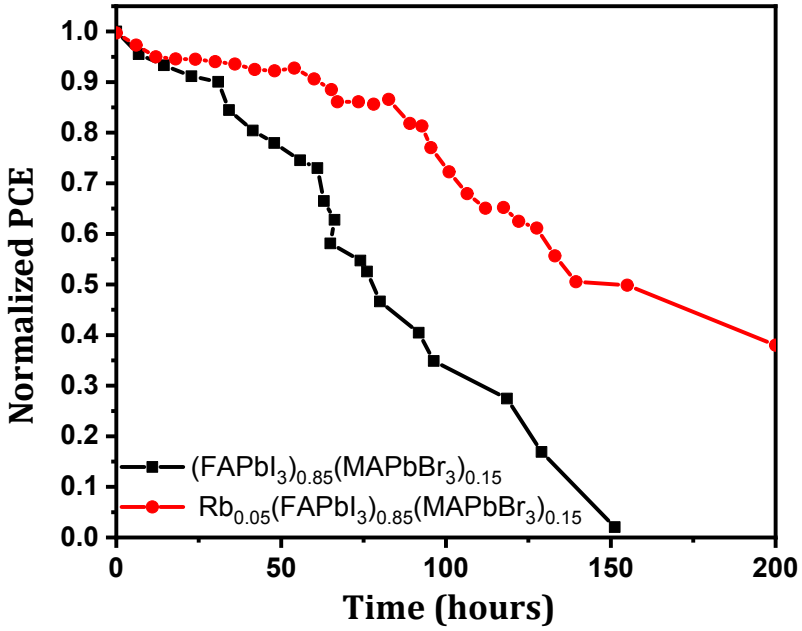

Table S1 Literature survey for pristine, doped SnO2 ETL and bilayer ETLs for planar perovskite solar cell

ETL	PSCs device configuration*	V_{OC} (V)	J_{SC} ($mAcm^{-2}$)	FF (%)	PCE (%)	Antisolvent	Ref
Doped and bilayer SnO_2							
SnO_2	FTO/SnO_2/$MAPbI_3$/spiro	1.11	23.27	67.0	17.21	N/A	J. Am. Chem. Soc. 2015, 137, 6730−6733.
SnO_2	FTO/SnO_2/FAMA/spiro	1.14	21.3	74.0	18.4	N/A	Energy Environ. Sci., 2015, 8, 2928—2934
SnO_2	FTO/SnO_2/CsFAMA/spiro	1.144	22.64	74	19.17	Diethyl ether	J. Mater. Chem. A, 2017, 5, 24790–24803
Li: SnO_2	FTO/Li:SnO_2/$MAPbI_3$/Spiro	1.106	23.27	70	18.20	Diethyl ether	Nano Energy 2016, 26, 208
Sb-doped SnO_2	ITO/Sb:SnO_2/$MAPbI_3$ /Spiro	1.06	22.6	72	17.2	Two steps N/A	ChemSusChem 2016, 9, 2689
Nb:SnO_2	FTO/Nb:SnO_2/$(FAPbI_3)_{0.85}$($MAPbBr_3)_{0.15}$ /Spiro	1.08	22.36	72.7	17.57	CB	ACS Appl. Mater. Interfaces 2017, 9, 2421
Y: SnO_2	FTO/Y: SnO_2/$MAPbI_3$/Spiro	1.08	22.55	71	17.29	Diethyl ether	Small 2017, 13, 1601769
Mg:SnO_2	FTO/Mg:SnO_2/$MAPbI_3$/spiro	0.991	20.92	66.8	13.56	Two step	J. Mater. Chem. A 2016, 4, 8374
SnO_2/PVP	ITO/SnO_2/MAPbICl/spiro	1.15	21.74	80.9	20.23	N/A	Sci. Adv. 2017;3: e1700106
SnO_2/np-SnO_2 (cryogenic technique)	FTO/SnO_2/np-SnO_2/CsFAMA/spiro	1.14	23.5	80	21.4	N/A	Adv. Mater. 2018, 1804402
F:SnO_2 bilayer ETL	FTO/$(F:SnO_2)_{380-0.2}$/$(F:SnO_2)_{180-0.2}$/FAMA /spiro	1.13	22.92	78.05	20.20	CB	Nano Lett. 2018, 18, 3969−3977

MgO/SnO_2	FTO/ $MgO/SnO_2/MAPbI_3$/Spiro	1.10	22.7	73.0	18.23	CB	Adv. Sci. 2017, 1700031
SnO_2/SAM	FTO/SnO_2/SAM/$MAPbI_3$/Spiro	1.16	21.93	72.0	18.32	Ethyl ether	J. Mater. Chem. A 2017, 5, 1658
SnO_2/PCBM	FTO/ SnO_2/PCBM /$MAPbI_3$/ Spiro	1.11	21.41	76.0	18.17	CB	J. Mater. Chem. A, 2016, 4, 14276
SnO_2/PCBM	$FA_{0.83}Cs_{0.17}Pb(I_{0.6}Br_{0.4})_3$	1.14	19.8	75.0	16.9	N/A	NATURE ENERGY 2, 17135 (2017)
SnO_2/PCBM	$BA_{0.05}(FA_{0.83}Cs_{0.17})_{0.91}Pb(I_{0.8}Br_{0.2})_3$	1.14	22.7	80.0	20.8	N/A	NATURE ENERGY 2, 17135 (2017)
SnO_2/PCBM	FTO/SnO_2/PCBM/CsFAMA/ spiro	1.10	19.9	70.7	15.1	N/A	Science, 2016, 351, 6269
SnO_2/PCBM/PMMA	FTO/SnO_2/PCBM/PMMA/ $Rb_5Cs_{10}FAPbI_3$/spiro	1.080	25.06	75.5	20.35	CB	Science 10.1126/science.aat3583 (2018).
SnO_2/SnO_2	FTO/SnO_2/SnO_2/RbFAMA/ spiro	1.17	23.1	-	20.3	CB	Energy Environ. Sci., 2018, 11, 78-86
SnO_2/SnO_2 SC + CBD	FTO/ SnO_2/SnO_2 SC + CBD CsFAMA/spiro	1.18	22.37	77.	20.78	CB	Energy Environ. Sci., 2016, 9, 3128—3134
SnO_2 (commercial)	ITO/SnO_2/FAI:MABr:MACl/ spiro	1.12	23.86	80.6	21.6	Two step	Adv. Mater. 2017, 29, 1703852
E-SnO_2	FTO/E-SnO_2/CsFAMA/spiro	1.11	24.57	79.2	21.6	CB	NATURE COMMUNICATIONS | (2018) 9:3239
ZW-SnO_2 (CBD)	FTO/ZW-SnO_2/FAMA/spiro	1.16	23.6	78.4	21.43	CB	Energy Environ. Sci., 2018, 10.1039/C8EE02242A
TiO_2	$MA_{0.5}FA_{0.5}PbI_3$	1.063	24.39	74.87	19.41	Diethyl ether	Solar Energy 157 (2017) 853–859
a-TiO_2/a-SnO_2	FTO/a-TiO_2/a-SnO_2/ $CsI_{0.05}(FAPbI_3)_{0.85}(MAPbBr_3)_{0.15}$/	1.169	23.91	76.5	21.4	CB (1-aminoadamant	Adv. Energy Mater. 2018, 8, 1800794

	spiro					ane 1.5 mg/mL)	
a-TiO_2/a-SnO_2	FTO/ a-TiO_2/a-SnO_2/ $MAPbI_3$/spiro	1.20	22.9	76.4	21.1	Toluene	ACS Energy Lett. 2017, 2, 2667−2673
TiO_2/SnO_2 (mesoporous)	TiO_2/SnO_2 /mp-TiO_2/CsFAMA/spiro	1.14	23.6	77	20.8	CB	Adv. Energy Mater. 2018, 8, 1700677
Bilayer ETLs							
c-TiO_2	FTO/ c-TiO_2/CsFAMA/spiro	1.132	21.77	76.1	18.76	Diethyl ether	Energy Environ. Sci., 2018, 11, 960—969
TiO_2/IL	FTO/TiO_2-IL/$MAPbI_3$/PTAA	1.0994	22.44	78.72	19.42	Two-step N/A	Energy Environ. Sci., 2016, 9, 3071—3078
TiO_2/TiO_2 (ALD/SC)	FTO/TiO_2/TiO_2/$MAPbI_3$/ spiro	1.07	20.5	75.2	16.5	N/A	small 2017, 13, 1701535
TiO_2-ZnO	FTO/TiO_2/$MAPbI_{3-x}Cl_x$/ spiro	0.969	21.13	74.2	15.1	N/A	ACS Appl. Mater. Interfaces 2016, 8, 29580−29587
TiO_2/ZnO	FTO/ TiO_2/ZnO/$MAPbI_3$/ spiro	1.084	21.03	75.3	17.17	CB	J. Mater. Chem. A, 2015, 3, 19288–19293
Zn_2SnO_4	FTO/ Zn_2SnO_4/$FAMAPbI_3$/ spiro	1.036	24.72	78.15	20.02	Two step	ACS Energy Lett. 2018, 3, 2410−2417
TiO_2/SnO_2	FTO/ TiO_2/SnO_2/CsFAMA/CuPc/ Carbon	0.980	23.38	67.0	15.39	CB	J. Mater. Chem. A, 2018, 6,7409
ZnO NPc/TiO_2	FTO/ZnO/TiO_2/$MAPbI_3$/ spiro	1.06	18.89	71.95	14.14	Diethyl ether	RSC Adv., 2018, 8, 23019–23026
ZnO/AZO	FTO/ZnO/AZO/$MAPbI_3$/ spiro/MoO_3/Ag	1.09	20.58	19.55	16.07	N/A	arXiv:1708.03153 [physics.app-ph]
ZnO/MgO-EA^+ (planar)	FTO/ZnO/MgO-EA/$MAPbI_3$/spiro	1.10	22.46	74.12	18.32	Diethyl ether	Adv. Mater. 2018, 30, 1705596
ZnO/MgO-EA^+	FTO/ZnO/MgO-EA/mp-	1.12	23.08	77.56	20.05	Diethyl ether	Adv. Mater. 2018,

(mesoporous)	TiO_2/$MAPbI_3$/spiro						30, 1705596
ZnO/MgO-EA^+ (mesoporous)	FTO/ZnO/MgO-EA/mp-TiO_2/CsFAMA/spiro	1.12	23.86	78.91	21.08	Diethyl ether	Adv. Mater. 2018, 30, 1705596
SnO_2/MgO (champion)	FTO/SnO_2/MgO/$MAPbI_3$/ spiro	1.13	22.1	75.7	19.0*	Diethyl ether	Nano Energy 49 (2018) 290–299
TiO_2	FTO/TiO_2/ $Rb_{0.05}(FAPbI_3)_{0.95}(MAPbBr_3)_{0.05}$/PTAA	1.09	21.77	71.05	15.60	CB	In this work
TiO_2/SnO_2	FTO/TiO_2/SnO_2/ $Rb_{0.05}(FAPbI_3)_{0.95}(MAPbBr_3)_{0.05}$/PTAA	1.029	22.74	71.82	16.80	CB	In this work
TiO_2	FTO/TiO_2/ $Rb_{0.05}(FAPbI_3)_{0.95}(MAPbBr_3)_{0.05}$/PTAA	1.018	22.15	72.30	16.30	Diethyl ether	In this work
TiO_2/SnO_2	FTO/TiO_2/SnO_2/ $Rb_{0.05}(FAPbI_3)_{0.95}(MAPbBr_3)_{0.05}$/PTAA	1.045	23.13	73.42	17.74	Diethyl ether	In this work
TiO_2	FTO/TiO_2/ $Rb_{0.05}(FAPbI_3)_{0.95}(MAPbBr_3)_{0.05}$/PTAA	1.052	22.17	0.73	17.03	TFT	In this work
TiO_2/SnO_2	FTO/TiO_2/SnO_2/ $Rb_{0.05}(FAPbI_3)_{0.95}(MAPbBr_3)_{0.05}$/PTAA	1.085	23.30	0.83	20.98	TFT	In this work

Note: *Please consider the normal composition of each perovskite precursor. All devices were completed by Au top contacts if not mentioned. (i) FAMA: $(FAPbI_3)_{0.85}(MAPbBr_3)_{0.85}$ (ii)CsFAMA: $CsI_{0.05}[(FAPbI_3)_{0.85}(MAPbBr_3)_{0.85}]_{0.95,}$ (iii) RbFAMA: $RbI_{0.05}[(FAPbI_3)_{0.85}(MAPbBr_3)_{0.85}]_{0.95}$, spiro: spiro-OMeTAD*